Neutron-star astrophysics with GWs: neutron-star mountains, r-modes and post-merger signals

Michał Bejger

TNPI2023 / 11.10.23

INFN FERRARA

Outline

- ⋆ Astrophysical motivation
- ⋆ Methods and challenges
- ⋆ Current results and outlook

Continuous GW sources vs other types of sources

(Hokusai "The Great Wave off Kanagawa")

One-time cataclysmic events, e.g. last moments of binary systems of

- ⋆ black holes (GW150914 etc.) and neutron stars (GW170817),

(Shoson "Cranes landing")

Persistent phenomena, e.g.

- ⋆ rotating asymmetric neutron stars ("*gravitational pulsars*"),
- ⋆ low-mass binary systems,
- ⋆ boson clouds.

Neutron stars = very dense, magnetized stars

The most relativistic **material** objects in the Universe: compactness $M/R \simeq 0.5$, observed in all EM spectrum as pulsars, magnetars, in supernovæ remnants, in accreting systems, in double neutron star binaries...

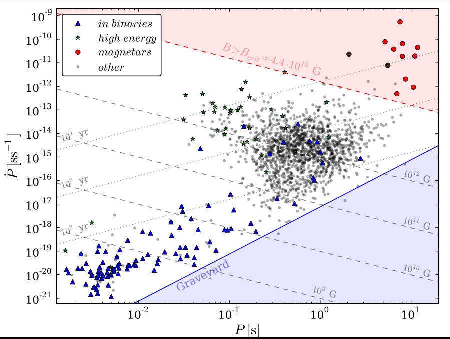

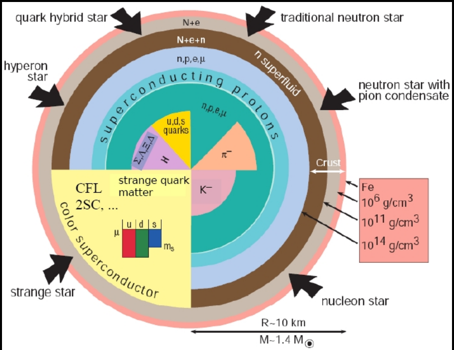

About 2500 NS observed to date, $\sim 10^8 - 10^9$ in the Galaxy.

Continuous GWs from spinning neutron stars

Characteristics:

- ⋆ Long-lived: $T > T_{obs}$,
- ⋆ Nearly periodic: $f_{GW} \propto f_{rot}$

Mechanisms that can create time-varying quadrupole moment:

- ⋆ "Mountains" (elastic and/or magnetic stresses, $f_{GW} = 2f_{rot}$),
- ⋆ Oscillations (r-modes, $f_{GW} = 4/3 f_{rot}$),
- ⋆ Free precession ($f_{GW} \propto f_{rot} + f_{prec}$)
- ⋆ Accretion (drives deformations from r-modes, thermal gradients, magnetic fields, $fGW \simeq f_{rot}$)

(see PASA **32**, 34 2015; Universe **5(11)**, 217 2019)

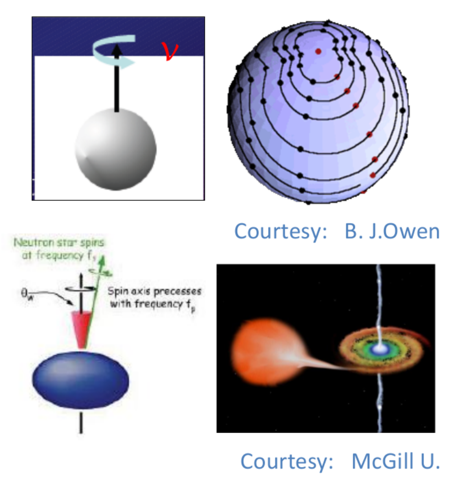

GW amplitude and the spindown limit

GW strain $h_0 = \frac{4\pi^2 G}{c^4} \frac{I_3 \epsilon f_{GW}^2}{d}$

with the distance d and the deformation $\epsilon = (I_1 - I_2)/I_3$. Depending on the dense matter model, $\epsilon_{max} = 10^{-3} - 10^{-6}$.

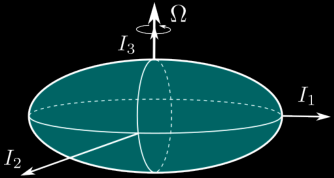

Rotational energy loss: $\dot{E}_{rot} \propto f\dot{f}$

Energy emitted in GWs: $\dot{E}_{GW} \propto f^6 I_3^2 \epsilon^2$

Spindown upper limit: observed spindown fully due to GWs, $\dot{E}_{rot} = \dot{E}_{GW}$:

Assuming the knowledge of I_3 and d

$\rightarrow$ upper limit $h_0^{sd} = \frac{1}{d}\sqrt{\frac{5G}{2c^3}\frac{|\dot{f}|}{f} I_3}$

$$\epsilon_{\rm sd} = 0.237\, I_{38}^{-1} \left[\frac{h_{\rm sd}}{10^{-24}}\right] \left[\frac{\rm Hz}{f_{\rm rot}}\right]^2 \left[\frac{d}{1\rm kpc}\right]$$

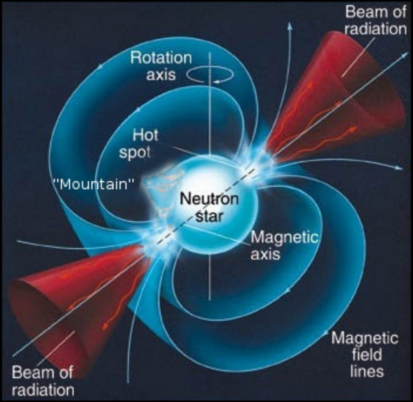

”Collider” vs ”table top” experiments

- $\star$ Many potential sources, but the GW ‘engine‘ is not guaranteed
  - $\star$ ”opposite problem” to transient compact binary coalescences (BH events).

- $\star$ GW amplitude is small: $\lessapprox 10^{-25}$ vs 10^{-21} (GW140915)

- $\star$ Discovery of a persistent source will be the capstone of GW astronomy:
  - $\star$ repeatable studies,
  - $\star$ access to ‘cold’ dense-matter equation of state of NSs, but also
  - $\star$ testing GR (polarizations etc.),
  - $\star$ searches for dark matter & exotic particles,
  - $\star$ detectors’ calibration, ”distance ladder”/cosmography.

Example: a monochromatic signal

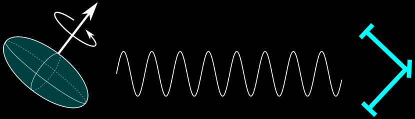

In this case a Fourier transform is sufficient to detect the signal (simplest matched filter method):

$$F = \left| \int_0^{T_0} x(t) \exp(-i\omega t) dt \right|^2$$

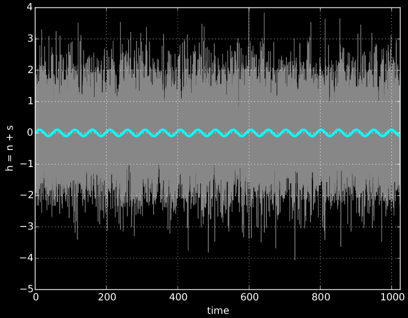

T_0 - time series duration, S_0 - spectral density of the data.

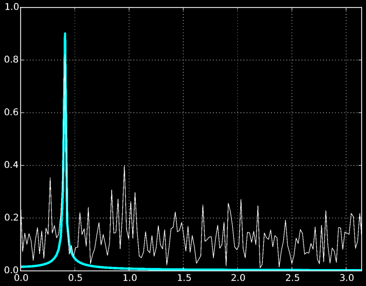

Signal-to-noise $SNR = h_0 \sqrt{\frac{T_0}{S_0}}$

Example: the $\mathcal{F}$-statistic

$\mathcal{F}$-statistic estimates how well the amplitude and phase modulated model matches the data $x(t)$

$$\mathcal{F} = \frac{2}{S_0 T_0} \left(\frac{|F_a|^2}{\langle a^2 \rangle} + \frac{|F_b|^2}{\langle b^2 \rangle} \right)$$

where S_0 is the spectral density, T_0 is the observation time, and

$$F_a = \int_0^{T_0} x(t) a(t) \exp(-i\phi(t)) dt, \qquad F_b = \ldots$$

$a(t)$, $b(t)$ - amplitude modulation functions that depend on the sources' sky position $(\alpha,\ \delta)$,

$\phi(t)$ - phase modulation function that depends on $(f, \dot{f}, \alpha, \delta)$

(PRD **58**, 063001, 1998)

All-sky CW search in LIGO O3a and O3 data

(PRD **103**, 064017 2021, `arXiv:2201.00697`)

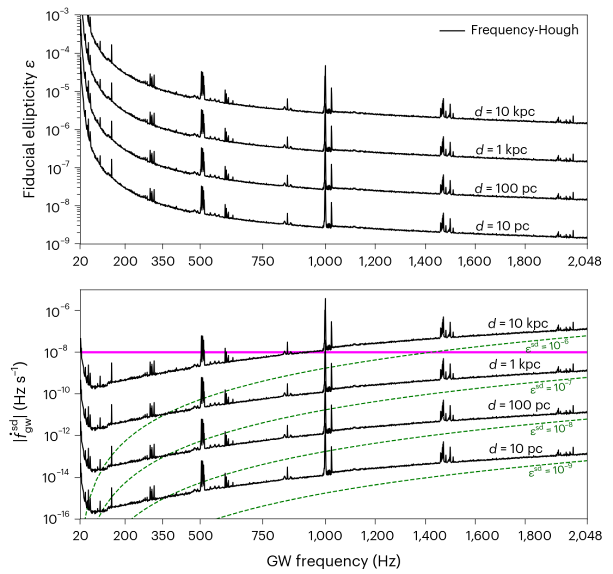

O3 search for GWs from known pulsars (ApJ **935**, 1 2022)

236 known pulsars analyzed at $l = m = 2$ and $l = 2, m = 1$ mode.

- ⋆ 23 targets surpass the spin-down limit. Highlights:
  - ⋆ Crab: less than $0.009\% \dot{E}_{rot}$ in GW,
  - ⋆ Vela: less than $0.052\% \dot{E}_{rot}$.

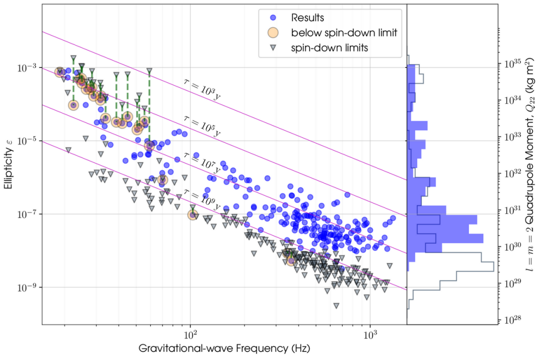

⋆ Two millisecond pulsars below the spin-down limit, including J0711-6830 with $f_{rot} \simeq 182$ Hz $\rightarrow$ ellipticity $\epsilon < 5.26 \times 10^{-9}$,

⋆ Limits for dipole GW emission in the Brans-Dicke theory.

Rossby waves in planetary atmospheres

- ⋆ Carl-Gustaf Rossby (1898 - 1957),
- ⋆ A type of inertial planetary wave, driven by Coriolis force (→ present in rotating systems),
- ⋆ On Earth, associated with high-altitude winds (→ jet stream),

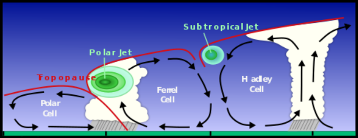

(Wikipedia)

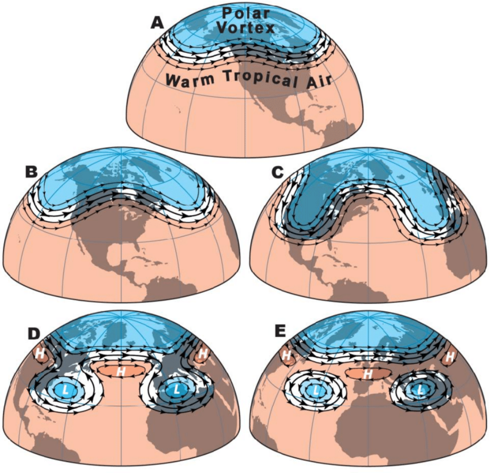

(S. Harris, AIMS Environmental Science 6(1):14-40 2019)

Rossby waves on neutron stars: r-modes

- ⋆ R-modes belong to a subset of inertial modes supported by rotation (Coriolis force as a restoring mechanism),
- ⋆ Retrograde in frame co-rotating with the star, prograde in inertial frame $\rightarrow$ unstable to Chandrasekhar-Friedman-Schutz (CFS) instability,
- ⋆ r-mode frequency in the rotating frame: $\omega_r = \kappa\Omega$, with $\kappa = \frac{2m}{l(l+1)}$.
- $\rightarrow$ for $l = m = 2$, $\omega_r = 2/3\Omega$,
- ⋆ In the inertial frame: $\omega_i = \omega_r - m\Omega = -4/3\Omega$.

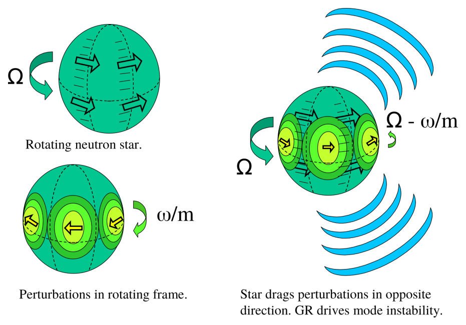

$l = m = 2$ mode frequency in Newtonian approximation is $\omega_i = 4/3\Omega$, in GR corrections related to NS mass and radius ($\rightarrow$ EoS):

$$\omega_i = \frac{4}{3}\Omega\left(1 + C_1\frac{GM}{Rc^2} - C_2\left(\frac{GM}{Rc^2}\right)^2\right),$$

where the $(1 + \dots)$ corrections are due to GR, rapid rotation, NS crust, matter stratification, magnetic fields... (Idrisy et al. 2015, Phys. Rev. D 91, 024001)

Relation between the GW and spin frequencies

The r-mode GW frequency f depends on the NS spin frequency ν and NS structure (e.g., Idrisy et al. 2015), which can be expressed as (Caride et al. 2019, Phys. Rev. D, 100, 064013):

$$
\begin{aligned}
f &= A\nu - B\left(\frac{\nu^2}{\nu_K^2}\right)\nu, \\
\dot{f} &= A\dot{\nu} - 3B\left(\frac{\nu^2}{\nu_K^2}\right)\dot{\nu}, \\
\ddot{f} &= A\ddot{\nu} - \left(3 + \frac{6}{n}\right)B\frac{\nu^2}{\nu_K^2}\ddot{\nu}.
\end{aligned}
$$

with constants A and B dependent on the EoS (assumption: they don't change between the glitches). A describes the effects of GR, B the effects of rotation; ν_K denotes the Keplerian (mass-shedding) frequency.

$$
\begin{aligned}
1.39 < & \quad A \quad < 1.57, \\
0 < & \quad B \quad < 0.195.
\end{aligned}
$$

PSR J0537–6910 a.k.a. the Big Glitcher

Young (1-5 kyrs) energetic X-ray pulsar in the LMC, rotating at $\nu = 62$ Hz:

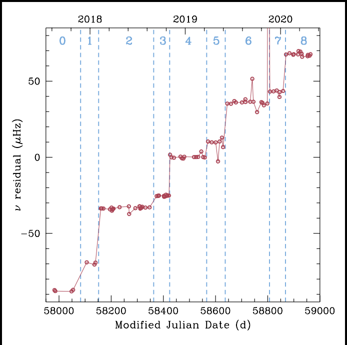

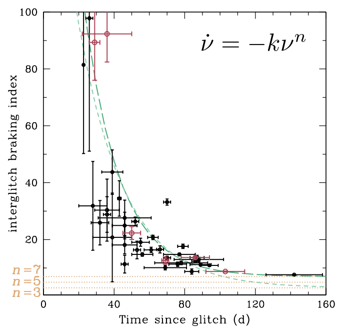

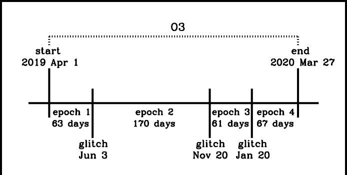

(Figs. 1 and 6 of Ho et al., 2020; Fig. 1, `arXiv:2104.14417`)

- ⋆ Timing $(\nu, \dot{\nu}, \ddot{\nu})$ solution provided by the NICER instrument, covering the O3 LIGO-Virgo observing run (Ho et al., 2020, MNRAS 498, 4605-4614).
- ⋆ Pulsar is associated with a SN remnant N157B → orientation: polarization $\psi = 2.2864$ and inclination angles $\iota = 1.522$.

Frequently glitching X-ray pulsar J0537-6910

J0537 is an energetic X-ray pulsar rotating at $f = 62$ Hz & rapidly spinning-down. Is some of the spin-down due to GW emission?

Search for r-modes, $f_{GW} \approx 4/3f \in 86 - 97$ Hz GW emission (ApJ **922**, 71 2021):

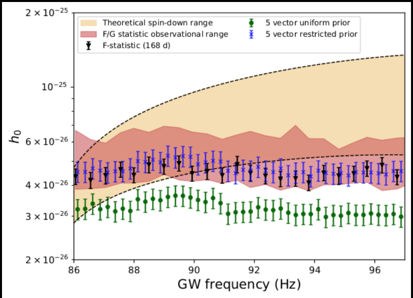

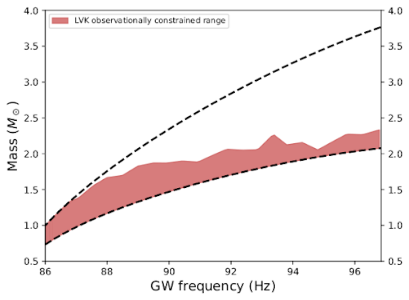

GW frequency of r-mode is a function of mass and radius of the NS → equation of state.

Sco X-1

Two searches for GWs from the low-mass X-ray binary Scorpius X-1 (NS in a binary system, with unknown orientation and frequency parameters):

- ⋆ PRD **106**, 062002 (2022) - Hidden-Markov model search
- ⋆ `arXiv:2209.02863` - semi-coherent CrossCorrelation search with stronger astrophysical model assumptions

Polarization-averaged upper limit reaches conservative torque balance prediction. ("accretion from binary companion is completely balanced by GWs")

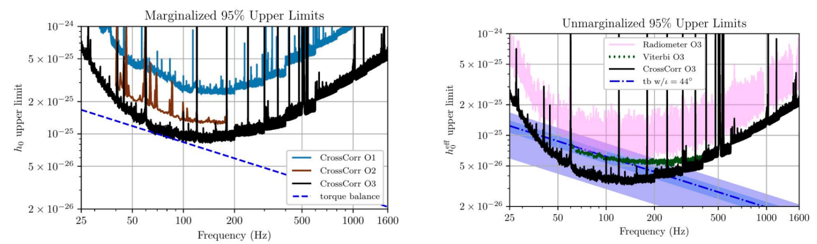

Search for post-merger signals (CQG **40** 215008 2023)

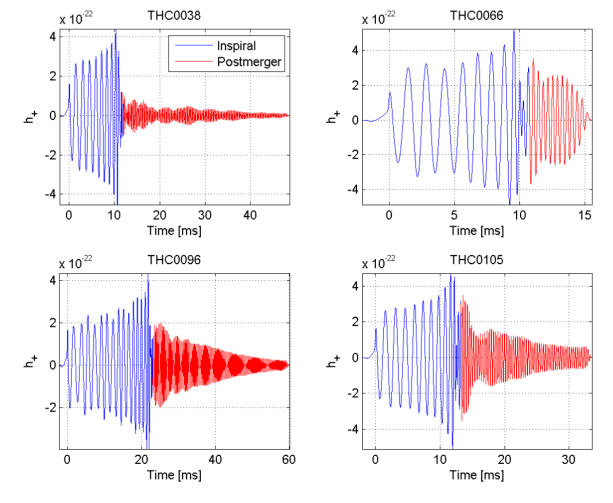

Waveforms consistent with GW170817 event, available in the 2nd release of CoRe database (CQG **40** 085011 2023)

Post-merger signals

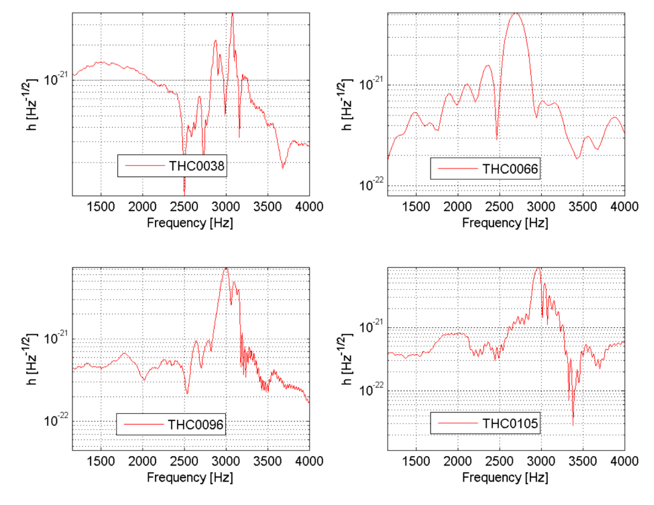

Postmerger spectra dominated by one frequency, f_{max}, related to the rotation of the bar-deformed high mass neutron star.

Post-merger signal: an approximation

Signal can be approximated by a sum of exponentially damped sinusoids

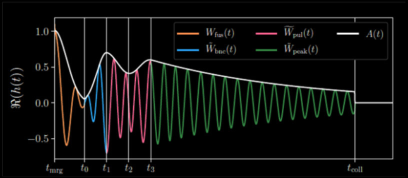

Morphology of NRPMw model (from Fig. 2 of Breschi et al.).

We approximate the postmerger signal by **one** damped sinusoid with 3 intrinsic parameters: frequency (f), frequency drift (γ), and damping time (τ) (we display here waveform of single $+$ or $\times$ polarization of the PM signal),

$$h(t) = h_o e^{-t/\tau} \cos(2\pi f t + 2\pi\gamma t^2 + \phi_o).$$

Post-merger signals

A universal relation between frequency f_{max} and an average compactness $\mathcal{C}$ of the binary neutron star:

$$f_{max} \simeq b_0 + b_1\mathcal{C} + b_2\mathcal{C}^2 \ \text{[kHz]},$$

where $b_0 = -3.12$, $b_1 = 51.90$ and $b_2 = -89.07$ and

$$\mathcal{C} = \frac{\bar{M}}{\bar{R}},$$

where $\bar{M}$ and $\bar{R}$ are average mass and radius of the binary repsectively.

$\bar{M}$ can be accurately determined from the inspiral phase and thus $\bar{R}$ can be determined from f_{max} estimate in the postmerger phase[1].

[1] Bose et al., Phys. Rev. Lett., 120:031102 (2018)

Triggers of the GW170817 postmerger search

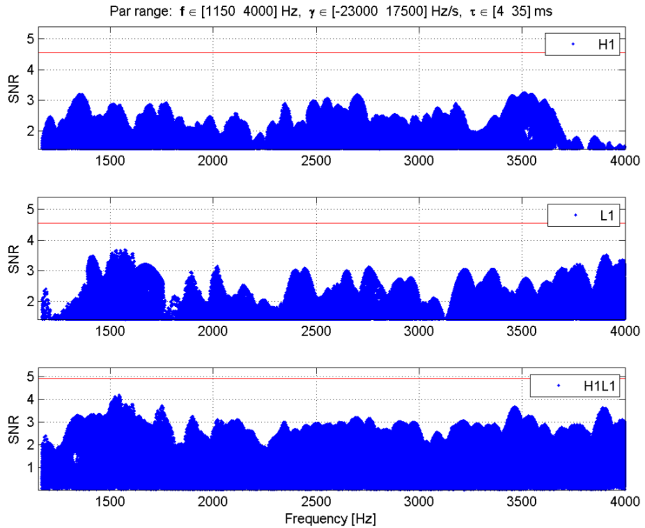

Horizontal red line — 1% false alarm probability threshold.

Other CW sources: low-mass primordial BHs

Inspiral of low-mass binary, with $\mathcal{M}_c = (m_1 m_2)^{3/5}/(m_1 + m_2)^{1/5} \approx 10^{-3} - 10^{-5}\ M_\odot$ results in slow evolution of chirp frequency $\approx$ CW signal

Evolution of GW frequency:

$$\frac{df}{dt} = \frac{96}{5}\pi^{8/3}\left(\frac{G\mathcal{M}_c}{c^3}\right)^{5/3} f^{11/3}$$

$\times$ (1 + PN corrections)

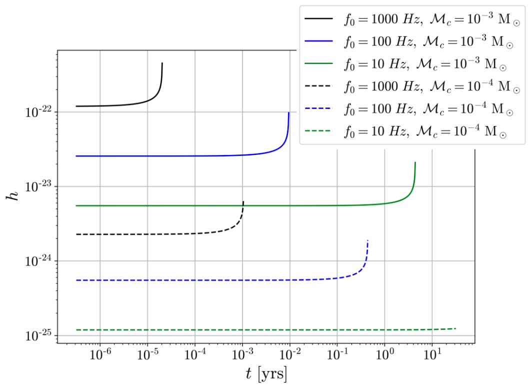

(Credit: Marc Andrés-Carcasona & Ornella Piccinni)

Other CW sources: boson clouds near BHs

- ⋆ CW emission from (hypothetical) light boson particles forming clouds around spinning BHs,
- ⋆ bosons will collide with each other over time, resulting in GW emission at almost constant frequency.

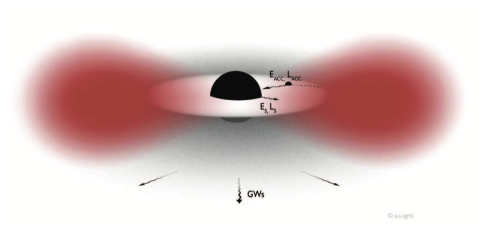

(Credit: Richard Brito, Vitor Cardoso, Paolo Pani)

(LVK analyses with O3 data: ”Search for continuous gravitational wave emission from the Milky Way center in O3 LIGO-Virgo data”, PRD **106**, 042003 2022, ”All-sky search for gravitational wave emission from scalar boson clouds around spinning black holes in LIGO O3 data”, PRD **105**, 102001 2022)

Summary and O4 outlook

- Searches for signals with more complicated morphology, transient aspects, loosely-coherent approach:
  - accounting for NSs glitches (sudden changes in spin frequency),
  - hierarchical follow-up of transient CW-like candidates,
  - using machine-learning algorithms.
  - NS spin frequency wandering,
  - mismatch between the GW frequency (and spindown) and the parameters inferred from EM observations
  - Focus on interesting targets like Sco X-1, supernovæ remnants (CasA, Vela Jr, G347, Crab)
  - GWs from r-modes and at multiple frequencies at once,
  - post-merger emission,
  - Dark matter constituents (also dark photon dark matter interacting directly with the detectors (as in PRD **105**, 063030 2022)
  - non-tensorial GWs.

(Astro)physics questions

- $\star$ Magneto-elastic 'mountains': elastic properties of the crust, braking strain,
- $\star$ Thermally induced quadrupole: accretion processes, heating reactions in the crust,
- $\star$ Instabilities (r-modes): heating & cooling, rotational evolution,
- $\star$ Superfluidity.

- $\star$ Conditions at birth: SN $\leftrightarrow$ NS deformation connection,
- $\star$ Long-term evolution of NS asymmetry,

- $\star$ Dark matter: PBHs, boson clouds, dark photons…

See Haskell & Bejger, Nature Astronomy (2023):
`https://rdcu.be/dmIeq`

Extra slides

O3 narrowband known pulsars search (ApJ **932**, 133 2022)

Usually assumed that GW signal is phase-locked with the pulsar EM emission.

Here, a small possible mismatch between the assumed and true signal phase evolution:

$\Delta f_{gw} = f_{gw}\,(1+\delta)$,
$\delta \sim 10^{-3} - 10^{-4}$

- ⋆ 18 pulsars, 7 surpassing the spin-down limit,
- ⋆ 6 glitching pulsars targeted for long-duration (hours-months) transient GWs

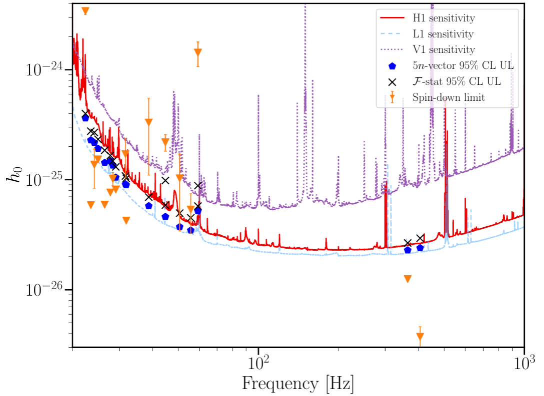

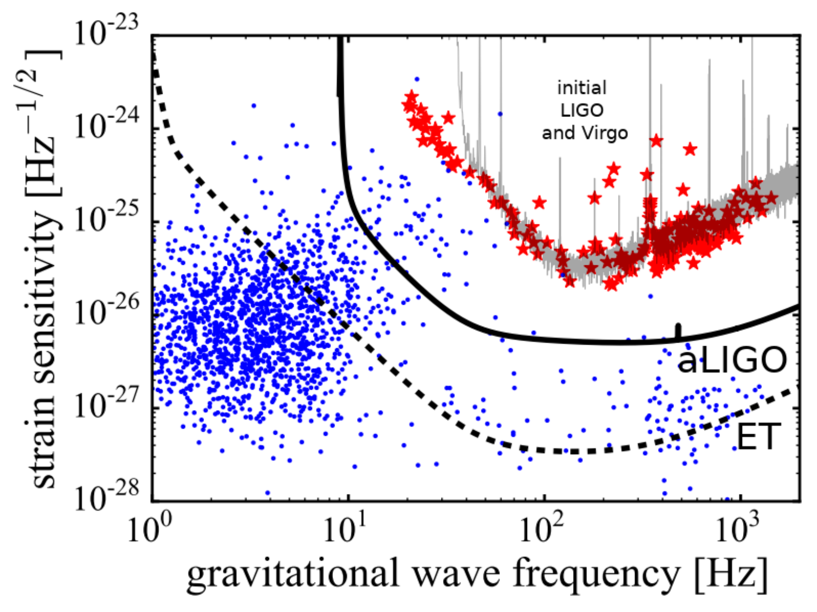

(PASA **32**, 34, 2015)

Example: computational cost for an all-sky search

In order to optimally cover a range of $(f, \dot{f}, \alpha, \delta)$ parameters,

$$\text{computing power} \propto \underbrace{T_0^2}_{\dot{f}} \times \underbrace{T_0^{[0-3]}}_{\alpha,\delta} \times \underbrace{T_0 \log(T_0)}_{f \text{ by FFT}} = T_0^{[3-6]} \log(T_0).$$

(see PRD **90**, 122010, 2014). Coherent search of $T_0 \simeq 1\, yr$ of data would require zettaFLOPS (10^{21} FLOPS) scale computers → currently impossible ☹

Solution: divide data into shorter length time frames ($T_s \simeq$ days)

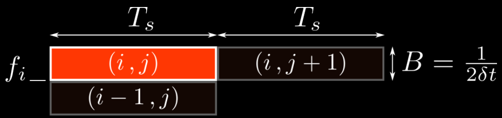

⋆ Perform a search in narrow frequency bands: sampling time $\delta t = 1/2B$, number of data points $N_p = T_s/\delta t = 2T_sB$

→ feasible on a petaFLOP computer.

Second stage: look for coincidences between different T_s segments.

Third stage: Analyze interesting outliers ("targeted search").

O3 constraints on boson clouds

"Search for continuous gravitational wave emission from the Milky Way center in O3 LIGO-Virgo data", PRD **106**, 042003 2022

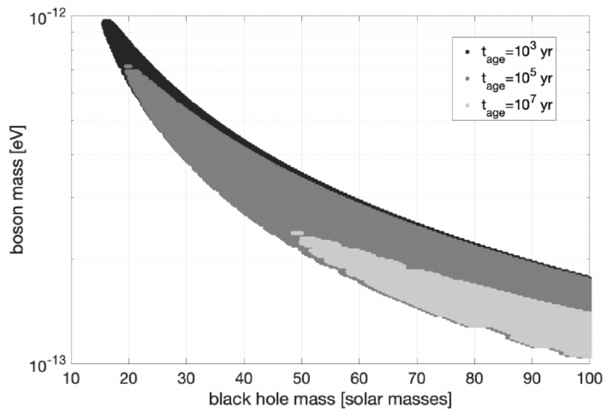

Constraints in the BH mass–boson mass plane for sources at the Galactic center. Clouds with different ages are considered (younger clouds emit stronger GWs). Shaded areas are excluded by observations.